Optical Materials 147 (2024) 114708

Contents lists available at ScienceDirect

Optical Materials

journal homepage: www.elsevier.com/locate/optmat

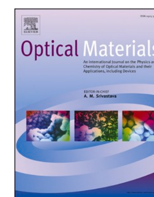

Research Article

Tuning of the Berreman mode of GaN/$Al_xGa_{1-x}N$ heterostructures on sapphire: The role of the 2D-electron gas in the mid-infrared

A. Bile [a,*], M. Centini [a], D. Ceneda [a], C. Sibilia [a], A. Passaseo [b], V. Tasco [b,1], M.C. Larciprete [a]

[a] Department of Basic and Applied Sciences for Engineering, Sapienza University of Rome, Via Scarpa 14, 00161, Rome, Italy
[b] CNR NANOTEC Institute of Nanotechnology, 73100, Lecce, Italy

ARTICLE INFO

Keywords:
AlGaN/GaN heterostrctures
Bidimensional electron gas effect
Berreman mode
ENZ materials
MIR technology

ABSTRACT

We investigated the mid-infrared optical properties of GaN/$Al_{(x)}Ga_{(1-x)}N$-type heterostructures on sapphire substrate grown by the Metal-Organic Chemical Vapor Deposition. We show how the polarization-dependent reflection spectrum is affected by the presence of the strain-induced 2D electron gas at the interfaces between $Al_{(x)}Ga_{(1-x)}N$ and GaN layers. In particular, we show that the 2D electron gas contribution, modeled from its density and transport properties, can play a relevant role at the Berreman mode excitation condition. In this framework, our results offer an advanced approach for the optimization and design of GaN-based broadband optoelectronic and energy management devices.

1. Introduction

The interest in the electromagnetic properties of GaN/$Al_xGa_{(1-x)}N$ heterostructures extends over a broad band from the visible/near UV to the GHz regimes [1,2]. Thanks to the formation of a strain-induced thin electron gas layer at GaN/AlGaN interface [3] and to the large energy gap, it is possible to design GaN-based optoelectronic devices for a huge number of applications where ultrafast, low-losses electronics can be combined to state of the art optical devices. For instance, GaN high-electron mobility transistors (GaN HEMTs [4]) have shown superior performance in various high-efficiency high power density applications and, at the same time, GaN technology has enabled the development of compact, low-cost blue and violet lasers [5]. Moreover, its high second-order nonlinear response combined with the ability to tailor the effective dispersion in multilayer structures provided fertile ground for the design of nonlinear frequency conversion devices, for example [6–8].

One of the promises of gallium and aluminum nitrides is the prospect of forming heterostructures for electronic and photonic applications. More recently GaN-based heterostructures have been intensively investigated also in the middle (mid-IR) and extreme infrared regions (up to THz) [9–11]. Indeed, being a polar material, GaN shows a negative permittivity in the mid-IR between the longitudinal optical (LO) and transverse optical (TO) phonon frequencies, called Reststrahlen band (RB) [12]. The interest in this region stems from the fact that the RB is a low-loss frequency band with negative permittivity enabling surface phonon polaritons (SPhP) excitation for enhanced material-light interactions [13]. Moreover, polar materials at the LO phonon frequency, are characterized by a vanishing real part of permittivity and a very small imaginary part [14] acting as a natural epsilon-near-zero (ENZ) material. This behavior opens the way to a huge number of potential IR applications ranging from high-field confinement for enhanced spectroscopy [15,16] and nonlinear interactions [17–19] to tailored heat near- and far-field radiative heat transfer [20] and radiative cooling [21]. However, as in HEMT electronic devices, in multilayer systems the internal (spontaneous and piezoelectric) field induce the formation of 2D electron gas (2DEG) at each interface that contributes to the modulation of the structures electromagnetic properties. Considering its typical electron density and mobility [22], the 2DEG plays a main role up to the THz regime and it becomes negligible in the optical range. For the same reason we expect a weak effect in the IR for free propagating fields, however, a relevant contribution might appear when surface phonon polaritons are excited. In particular, we show that the effect of the 2DEG is not negligible for free-space propagating field around the ENZ condition if the heterostructure is deposited on a polar substrate (i.e. sapphire). Indeed, it is well known that in this

* Corresponding author.
E-mail address: alessandro.bile@uniroma1.it (A. Bile).

[1] V. Tasco is currently seconded at the European Research Council Executive Agency of the European Commission. Her views expressed in this paper are purely those of the writer and may not in any circumstance be regarded as stating an official position of the Euopean Commission.

https://doi.org/10.1016/j.optmat.2023.114708
Received 30 October 2023; Received in revised form 1 December 2023; Accepted 6 December 2023
0925-3467/© 2023 The Authors. Published by Elsevier B.V. This is an open access article under the CC BY license (http://creativecommons.org/licenses/by/4.0/).

condition it is possible to excite Berreman modes [23] at the surface of the substrate as long as the LO phonon resonance of the ENZ material falls in the RB of the substrate. The Berreman mode is a leaky propagating surface mode where the ENZ material (i.e the GaN based heterostructure around the LO phonon resonance) enables evanescent wave coupling of an incident free-space propagating field to the surface polariton mode of the substrate and vice versa. We note that the Berreman mode can be excited only with p-polarized fields. Thus, its excitation is observed in the far field reflection spectra as a sharp polarization-dependent dip, revealing energy absorption from the substrate. Besides applications as tunable IR filters [24], the high field localization related to the excitation of the Berreman mode has been used to enhance nonlinear second harmonic generation in the mid-IR [25].

In the present work, we investigate the IR reflectance of GaN/$Al_xGa_{(1-x)}N$ heterostructures grown on a sapphire substrate using Metal-Organic Chemical Vapor Deposition (MOCVD) with the aim to evaluate the contribution of the 2DEG on the tunability and modulation depth of the Berreman mode. The experimental measurements were analyzed numerically using the generalized 4 × 4 transfer matrix method for anisotropic materials [26]. A thin (2 nm) layer with an effective complex dielectric permittivity was considered before every GaN/$Al_xGa_{(1-x)}N$ interface (in Ga-face structures, as resulted with MOCVD growth, a 2DEG is confined in the layer with the smaller bandgap close to the interface [27]) including a high-frequency Drude-conductivity of 2D electrons (2DEG). In order to deeply understand the effect of the 2DEG we consider as a first step a sample with only one GaN/AlGaN interface. We discuss the discrepancies between experimental and theoretical results highlighting the role of the 2DEG, using the electron density and transport properties retrieved from the literature [10,22]. Then we study a complex heterostructure to investigate the effect on a multilayer system. We chose as an example a typical multilayer micro-cavity designed for visible applications. A complete study of the properties in the extended visible/mid-IR range is important for nonlinear frequency conversion applications as well as for radiative cooling/energy management applications. However, it goes beyond the scope of this work. Here we focus on the mid-IR properties showing that the 2DEG contribution in the theoretical model improves the interpretation of experimental results and can be relevant in the design of multi-frequency, broadband devices including mid-IR surface wave excitation.

2. Results and discussions

To shed light on the effect of 2DEG, reflection spectra of GaN/AlGaN heterostructures on sapphire substrate have been acquired in the 400-1000 cm^{-1} range using a Bruker INVENIO-R FTIR spectrometer with an incidence angle of 15°. The characterization is conducted using one linear polarizer to address different polarization states of the incoming light ranging from s (0°) to p (90°). This setup allows us to excite the Berreman mode at the interface between the heterostructures and the substrate when the p-polarization is selected for the incident field. In the presence of this leaky surface mode we expect that the role of the 2DEG will be enhanced. Two samples have been investigated: the first one (sample A) consists in a typical HEMT structure where a single, well-defined 2DEG layer is formed at the GaN/AlGaN interface. As sketched in Fig. 1a, the 2DEG layer is located at the interface between the high-quality GaN buffer layer of 2000 nm and the 20 nm AlGaN layer with 30 % Al content. The high temperature (HT) AlN nucleation layer, directly grown on the Al_2O_3 substrate is polycrystalline [28] thus preventing the built up of the piezoelectric internal field and, consequently, any 2DEG at the interface between the AlN and the following high-quality GaN buffer layer. The second sample (B), depicted in Figure 1b, is a typical GaN/$Al_xGa_{(1-x)}N$ multilayer device operating as a microcavity in the visible range. Here a 2DEG sheet is expected at every GaN/$Al_xGa_{(1-x)}N$ interface, confined in the GaN layers and modulate by the different distribution of the strain field. We want to investigate the combined effect of multiple 2DEG sheets for the future design of broad-band GaN-based multifrequency devices operating from the near UV to the mid-IR. See the sample's fabrication methods paragraph for more details.

Experimental spectra for sample (A) and sample (B) for different incident filed's polarizations are reported in Fig. 2a and b. We note that the mid-IR spectra show many analogies. The excitation of the Berreman mode is clearly visible at 736 cm^{-1} for both sample (A) and sample (B). This condition is achieved around the $\omega_{LOz} = 732.5$ cm^{-1} phonon frequency of the GaN, associated to an ENZ condition. The sharp reflectivity valley, corresponding to the Berreman mode, can be strongly tuned with the polarization of the incoming light. Specifically, for p-polarized light (90 deg) the maximum depth is reached, achieving a corresponding gain factor Q = 53 for sample (A) and Q = 49 for sample (B). This reflectance dip completely disappears when the incoming light is s-polarized (0 deg). We note that the modulation range of the reflectance dip is decreased in sample (B). Both experimental spectra display the modulating region between 840 and 910 cm^{-1}, related to the anisotropy of the sapphire substrate. The use of sapphire as a substrate ensures that the GaN LO phonon is centered in the sapphire Reststrahlen band. Under this condition, the Berreman mode can be excited at the interface between sapphire and GaN. The choice of a different substrate, for example silicon carbide (SiC), would result into a different frequency range, i.e. SiC's Reststrahlen band 797-970 cm^{-1} [10,29]. As a

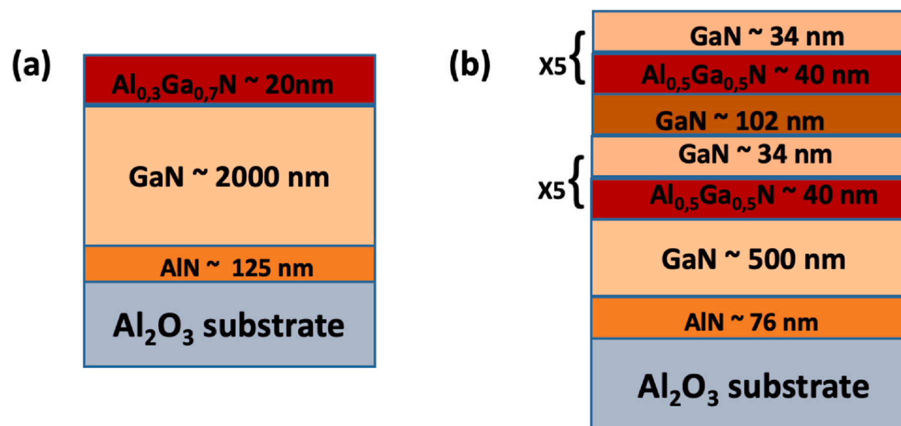

Fig. 1. a) sketch of Sample (A): a single 2DEG sheet is embedded between the $Al_{0.3}Ga_{0.7}N$ and the GAN layer. No 2DEG is expected at the interface between GaN and the AlN nucleation (polycrystalline) layer; b) sketch of sample (B) consisting of a typical multilayer stack operating in the visible range. A 2DEG sheet is expected at every GaN/$Al_xGa_{1-x}N$ interface.

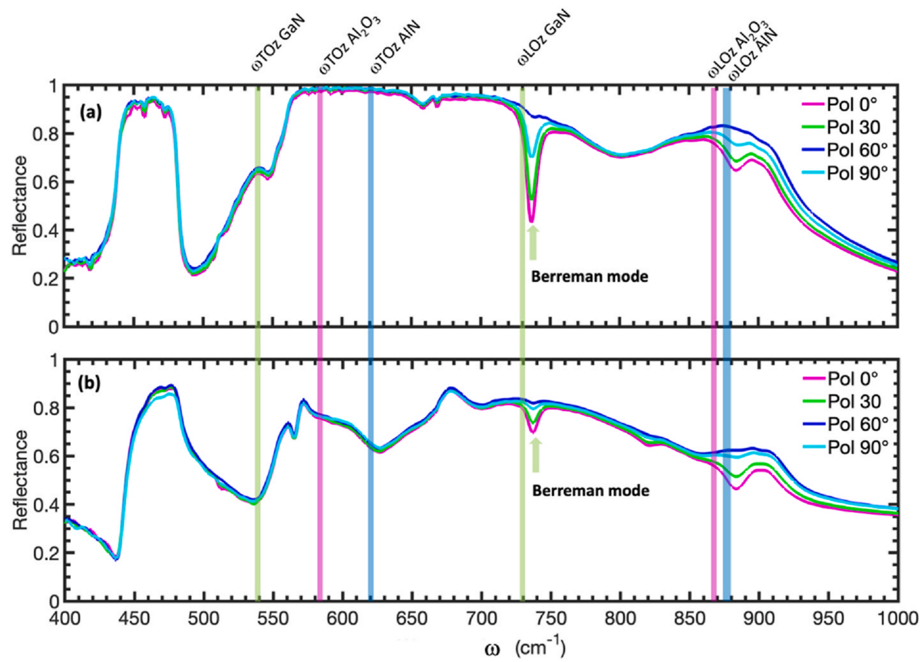

Fig. 2. Polarization-dependent reflection FTIR spectra measured at 15 deg incidence angle for (a), Sample (A) and (b), Sample (B) sketched in Fig. 1a and b. Polarization of the incident field was varied between 0° and 90° with a step value of 30°. As a reference we included a sketch of the RBs for sapphire (red top bar) and for GaN(blue top bar) to show that the Berreman mode, excited near the GaN LO phonon resonance, falls almost in the middle of sapphire's RB.

consequence, the GaN LO phonon would fall outside this band. However, SiC substrate can be used to efficiently excite the Berreman mode at interface with AlN (ωLO = 890 cm^{-1}) [29]. Other remarkable differences are due to the different contents of GaN and AlN. For instance in sample (A), Fig. 2a shows a deeper, almost polarization-independent, reflection minimum around 500 cm^{-1} (being $\omega_{TOx} = \omega_{TOy} = 537$ cm^{-1} for GaN) with respect to sample (B). On the other hand, sample (B) in Fig. 2b displays a deeper minimum with respect to sample (A) around 650 cm^{-1} ($\omega_{TOx} = \omega_{TOy} = 667$ cm^{-1} for AlN).

The investigation of the contribution of the 2DEG has been performed by comparison of the experimental data with the theoretical predictions. The reflectivity spectra of the samples were modeled using a 4 × 4 transfer matrix method for anisotropic multilayer stacks [26]. The dielectric permittivity tensors of GaN, as well as $Al_{(x)}Ga_{(1-x)}N$ layers and sapphire substrate, have been retrieved using phonon oscillator models and parameters reported in Ref. [13]. With respect to a previous work [10] where the effect of the 2DEG has been investigated in the Long wavelength IR (LWIR) here we considered anisotropic models for all the

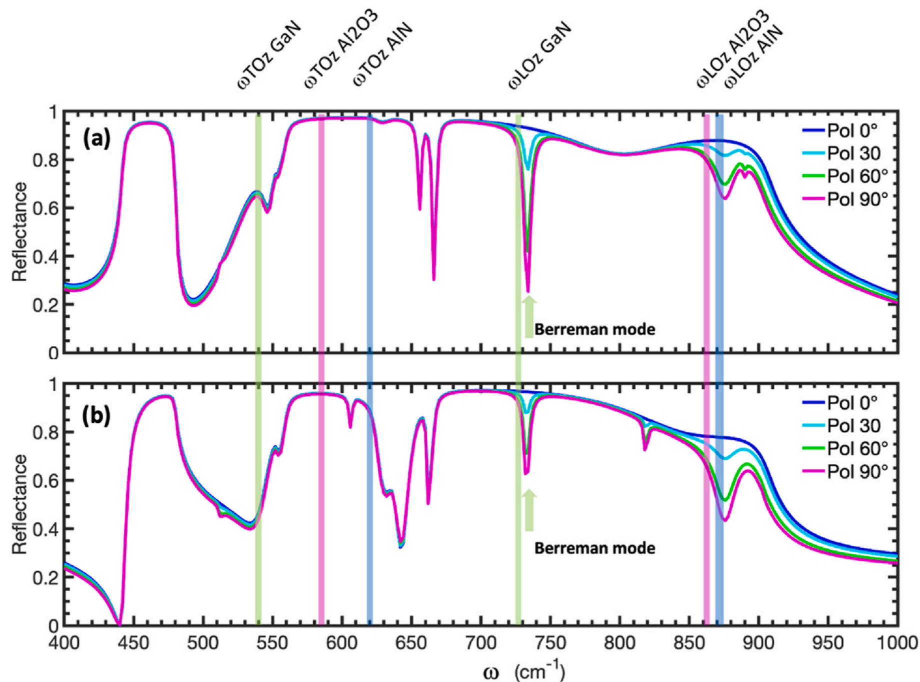

Fig. 3. Polarization-dependent theoretical reflection spectra for (a), Sample (A) and (b), Sample (B) sketched in Fig. 1a and b. Polarization of the incident field was varied between 0° and 90° with a step value of 30°.

layers with the exception of the first HT polycrystalline AlN layer which is, by definition, isotropic. As a first step we compare the experimental spectrum of both samples with the theoretical prediction obtained neglecting the 2DEG contribution. The obtained results, reported in Fig. 3 clearly show big discrepancies, mostly evident in the reflection dips. Moreover, according to theoretical calculations, the resonance associated with the GaN Berreman mode displays Q factors as high as 75 for sample (A) and 64 for sample (B), which are significantly higher with respect to the experimental results.

A better match between simulations and measurements can be obtained if the conducting interface due to the presence of a two-dimensional electron gas (2DEG) in the multilayer heterostructure is taken into account. In particular, its permittivity was constructed by considering the background of GaN permittivity and adding the 2DEG complex permittivity retrieved from the effective conductivity computed using the Drude model:

$$\sigma(\omega) = \frac{e^2 N_s \tau}{m_e} \bullet \frac{1}{(1 - i\omega\tau)\,\mathrm{r}} \tag{1}$$

where e is the electron charge, N_s is the 2DEG surface carrier density, m_e is the effective electron mass, r is an effective spatial parameter depending on the electron mobility μ, τ is the relaxation time defined as $\tau = \frac{m_e \mu}{e}$. Sample (A) has been specifically fabricated with the aim to maximize electron density and mobility of the 2DEG, thus we modeled it using the typical experimental data from literature [10,21], reported in Table 1

Fig. 4a and b depict the theoretical reflection spectra obtained by taking into account the 2DEG contribution. We report experimental and theoretical results in the same plot for p- (Fig. 4a) and s- (Fig. 4b) polarized incident fields. When comparing the previous theoretical results (Fig. 3a) a general improvement in experimental vs. theory agreement is more evident. We note that the depth of the reflectivity dips corresponding to the TO AlN phonon gets reduced since the gas introduces a reflectivity increase of the overall structure before reaching the deep layer where the AlN is located. More remarkably, the polarization tunability of the Berreman mode excited around the LO GaN phonon is also modified by the introduction of 2D electron gas.

The contribution of 2DEG to the theoretical model was also assessed by calculating the coefficient of determination between simulation and experimental curves: for sample A, the coefficient increases from 0.85 (without 2DEG) to 0.99 (with 2DEG) for s-polarized and from 0.35 to 0.75 for p-polarized incoming light. An improved agreement between theoretical calculations and experimental measurements within this spectral region is also evidenced by the Q-factor value calculated in correspondence of the Berreman mode frequency: when the 2DEG layer is taken into account, the Q-factor drops to 48, resulting in a good match between theoretical and experimental. The results obtained show that the effect of 2DEG is not negligible, and its effects can significantly affect the spectrum of AlGaN/GaN heterostructures, decreasing the contrast of resonances and their Q-factors.

To shed light on the 2DEG effects on the sample (B)'s reflection spectra, we added a 2DEG layer between every AlGaN/GaN interface. However, for structures with multiple interfaces and very small layer thickness (as in sample B), it must be considered that the different distribution of the strain field (that modulate the piezoelectric internal field) strongly influences the density and mobility of the 2DEG, with a significant reduction of both parameters, that must be taken into account [30,31]. Indeed, we found a good agreement with experimental results if the electron density and the mobility of the 2DEG are reduced by one order of magnitude. We report in Table 2 the parameters used for calculations. We note that the 2D electron density and the mobility are reduced of two orders of magnitude with respect to the previous sample.

Table 1
Two-dimensional electronic gas (2DEG) performance data [12,22].

N_e (10^{16} m^{-2})	μ (10^{-1} m^2/V·s)	m_e (10^{-31} kg)
8.3	1.9	3.1

In Fig. 5 a-b we report in the same plot experimental and theoretical results for p- (Fig. 5a) and s- (Fig. 5b) polarized incident fields, respectively. We note that also for this sample the contribution of the 2DEG is not negligible, especially in the low reflectance peaks. Considering 2DEG, the agreement between experimental and theoretical prediction is sensibly improved and the Berreman mode Q factor is now 49. Also in this case, the contribution of 2DEG to the theoretical model was also assessed by calculating the coefficient of determination between simulation and experimental curves: for sample B, the coefficient increases from 0.33 (without 2DEG) to 0.60 (with 2DEG) for s-polarized and from 0.48 (without 2DEG) to 0.62 (with 2DEG) for p-polarized incident light.

Such an extra parameter affecting overall reflectivity features can bring new possibilities to engineer polarization for optoelectronic devices implemented with aluminum and gallium nitrides.

3. Conclusions

In this work, we touched on the mid-IR spectral features of GaN/$Al_xGa_{(1-x)}N$ heterostructures. Experimental findings along with the theoretical model highlight the effect of the two-dimensional electron gas (2DEG) formed at the AlGaN/GaN interfaces on the mid-IR reflection spectra. Because of the relatively low density and conductivity, 2DEG is usually neglected in this wavelength range. However, our study reveals that it can play a non-negligible role in the reflectivity minima related to material phonon resonances. More specifically, if leaky surface modes, (i.e. Berreman modes), are excited, the 2DEG contribution emerges as a critical factor in determining the infrared reflectivity features. These findings offer new routes for material characterization and design of IR optoelectronic devices. The investigated sharp resonances in the mid-IR could be employed to implement sensing devices based on far-field configuration. Moreover, they could be used in combination with the tailored optical properties in the visible/near-IR for radiative cooling and enhanced nonlinear frequency conversion.

4. Fabrication methods

Epitaxial films used in this study were directly grown on (001) c-plane Al_2O_3 substrates in a low-pressure MOCVD system using standard precursors and H_2 as a carrier gas. The first sample, sample (A), was realized to clearly investigate the effect of the 2DEG on a simple system consisting of only one, well-defined 2DEG layer at the GaN/AlGaN interface. A 125 nm thick high temperature (HT) AlN nucleation layer was directly grown on the Al_2O_3 substrate at 1150 °C, followed by a high-quality GaN buffer layer of 2000 nm and around 20 nm of AlGaN layer with 30 % Al content (Fig. 1a), grown at the same temperature. The growth on HT AlN nucleation layer allows a strong reduction in the GaN epilayer mosaicity with the disorder induced by the large mismatch with the substrate concentrated only in the first 50 nm, rapidly decreasing for thicker growth [26]. This results in a high-quality GaN layer even for small thickness with narrow x-ray diffraction (XRD) reflection peak suitable for the growth of the AlGaN/GaN multistacks [28].

A second Sample (sample (B), sketched in Fig. 1b) consisting of a 76 nm thick high temperature (HT) AlN nucleation layer directly grown on the Al_2O_3 substrate at 1150 °C, followed by a high-quality GaN buffer layer of 500 nm and by a AlGaN/GaN microcavity stack was realized to investigate the mid-IR optical properties in a typical multilayer device operating in the visible range. More in detail the microcavity consists of a 102 nm GaN layer sandwiched between 5 + 5 pairs of 40/34 nm thick AlGaN/GaN layer (50 % Al content) grown at 1180 °C acting as Bragg mirrors. These typical geometrical parameters correspond to a half-wavelength GaN microcavity tuned around 450 nm wavelength.

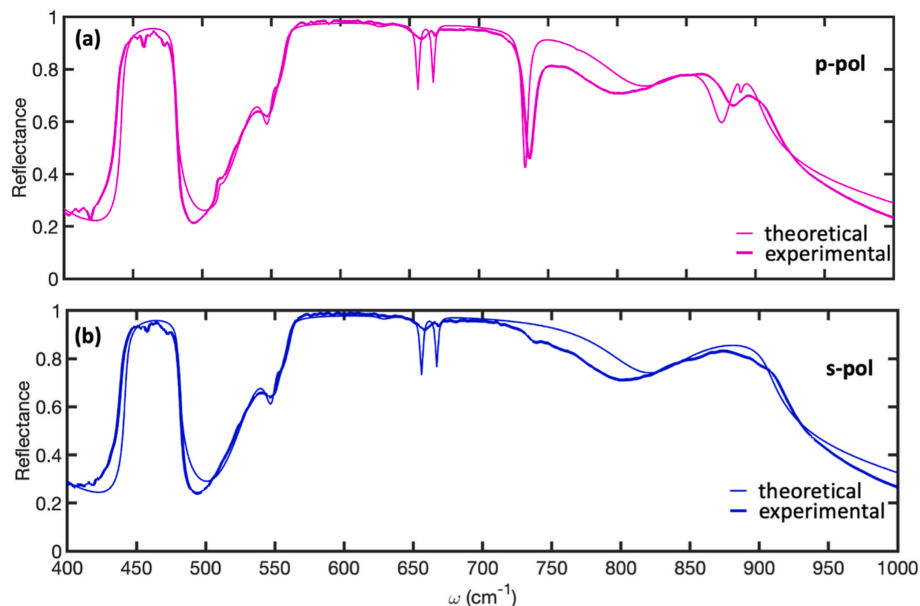

Fig. 4. Experimental (thick line) and theoretical (thin line) reflectance spectra of sample (A) for p- (a) and s- (b) polarized incident fields. The theoretical results are obtained including the contribution of the 2DEG.

Table 2
Two-dimensional electronic gas (2DEG) parameters used to model sample b interfaces.

N_e (10^{14} m^{-2})	μ (10^{-3} m^2/V·s)	m_e (10^{-31} kg)
4.3	1.6	3.1

5. Experimental methods

A Bruker INVENIO-R FTIR spectrometer equipped with a globar as a radiation source and a KBr beam splitter was used to carry polarization-dependent reflectance measurements of the samples. Reflection spectra at 15° angle of incidence were obtained using Fourier transform infrared (FTIR) system in the frequency of 400–1000 cm^{-1}, using a resolution step size of 3 cm^{-1}. The instrument operates at room temperature (about 300K) in the spectral region between 400 and 8000 cm^{-1}. The FTIR system is equipped with a variable angle reflection stage, while the incidence angle was fixed at 15 deg. The input light polarization can be varied using a motorized wide-range holographic grid polarizer. All measurements were normalized using a gold reference mirror as a background signal, under the same experimental conditions. The intensity of IR radiation was measured by a DLaTGS pyroelectric detector.

6. Theoretical methods

The reflectivity spectra of the samples were modeled using a 4 × 4 transfer matrix method for anisotropic materials [25]. The numerical method allows the calculation of the four reflection coefficients for the multilayer structure, namely r_{ss}, r_{pp}, r_{sp} and r_{ps}, where ss (pp) stand for s- (p-) polarization of incident field and s- (p-) polarization for detected

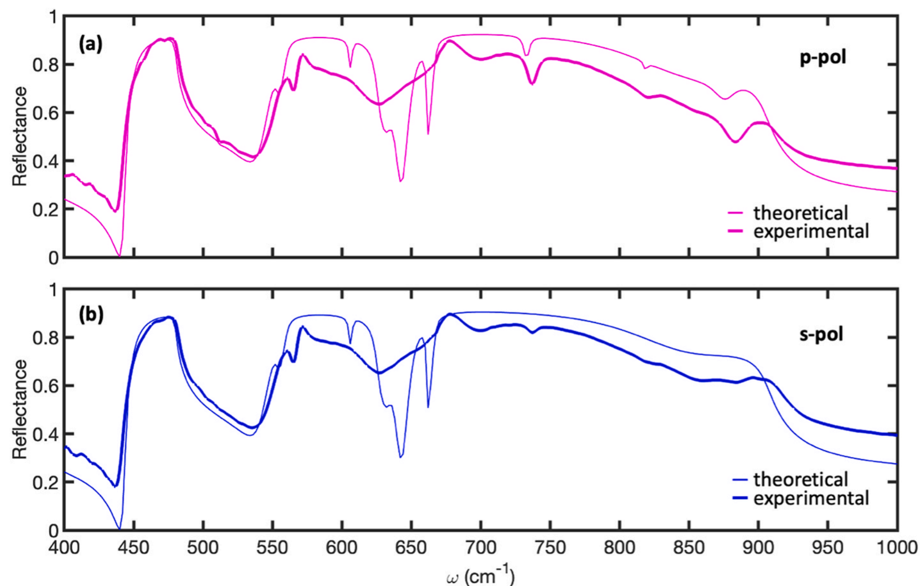

Fig. 5. Experimental (thick line) and theoretical (thin line) reflectance spectra of sample (B) for p- (a) and s- (b) polarized incident fields. The theoretical results are obtained including the contribution of the 2DEG.

field respectively while sp (ps) represent the cross-polarized reflectivity. In our experimental setup we only select the incident field polarization angle φ_{in}, where $\varphi_{in} = 0$ (90) stands for s-pol (p-pol). Since all the reflected signal is collected, we model the reflected field as follows. First, we evaluate the s- and the p-components of the reflected field:

$$E_s = r_{sp}\cos(\varphi_{in}) + r_{ss}\sin(\varphi_{in}) \tag{2a}$$

$$E_p = r_{pp}\sin(\varphi_{in}) + r_{ps}\cos(\varphi_{in}) \tag{2b}$$

Then we calculate the reflectance as:

$$R = |E_s|^2 + |E_p|^2 \tag{3}$$

The 2DEG effective conductivity is computed using the previously mentioned Drude model formula in Eq. (1) from which we obtain a complex effective dielectric permittivity affecting the in-plane response:

$$\varepsilon_{\parallel}^{cond} = \frac{i\sigma}{\varepsilon_0\omega} \tag{4}$$

The effective permittivity of the layer which model the 2DEG is obtained by summing Eq. (4) to the background permittivity. According to Refs. [27–30], the 2DEG is assumed to be in the GAN, approximately 1–2 nm before the interface. Thus, the contribution of the 2DEG is taken into account by considering a 2 nm layer having an effective complex dielectric permittivity given by:

$$\varepsilon_{\parallel}^{2\ DEG} = \varepsilon_{\parallel}^{GaN} + \varepsilon_{\parallel}^{cond} \tag{5a}$$

$$\varepsilon_{\perp}^{2\ DEG} = \varepsilon_{\perp}^{GaN} \tag{5b}$$

Finally, the 2DEG is included in the 4×4 transfer matrix method as a standard layer, placed 2 nm before the borders of every GaN layer sandwiched between $Al_{(x)}Ga_{(1\text{-}x)}N$ layers.

CRediT authorship contribution statement

A. Bile: Conceptualization, Data curation, Formal analysis, Investigation, Writing – original draft, Writing – review & editing. **M. Centini:** Conceptualization, Methodology, Supervision, Validation, Writing – original draft, Writing – review & editing. **D. Ceneda:** Software, Visualization. **C. Sibilia:** Visualization. **A. Passaseo:** Resources, Supervision, Writing – original draft, Writing – review & editing. **V. Tasco:** Visualization, Resources. **M.C. Larciprete:** Conceptualization, Methodology, Supervision, Writing – original draft, Writing – review & editing.

Declaration of competing interest

The authors declare that they have no known competing financial interests or personal relationships that could have appeared to influence the work reported in this paper.

Data availability

Data will be made available on request.

References

[1] R.J. Kaplar, et al., ECS J. Solid State Sci. Technol. 6 (2017) Q3061.
[2] S. Nakamura, et al., High-power GaN P-N junction blue-light-emitting diodes, Jpn. J. Appl. Phys. 30 (1991) L1998.
[3] F. Bernardini, V. Fiorentini, Macroscopic polarization and band offsets at nitride heterojunctions, Phys. Rev. B 57 (16) (1998) R9427.
[4] U.K. Mishra, P. Parikh, Y.-F. Wu, AlGaN/GaN HEMTs-an overview of device operation and applications, Proc. IEEE 90 (6) (2002) 1022–1031.
[5] Y. Sun, K. Zhou, M. Feng, et al., Room-temperature continuous-wave electrically pumped InGaN/GaN quantum well blue laser diode directly grown on Si, Light Sci. Appl. 7 (2018) 13.
[6] Y. Zheng, C. Sun, B. Xiong, et al., Integrated gallium nitride nonlinear photonics, Laser Photon. Rev. 16 (2021), 2100071.
[7] M.C. Larciprete, M. Centini, A. Belardini, et al., *Second harmonic generation in GaN/$Al_{50}Ga_{50}N$ films deposited by metal-organic chemical vapor deposition*, Appl. Phys. Lett. 89 (2006) 13.
[8] E. Fazio, et al., Measurement of pure Kerr nonlinearity in GaN thin films at 800 nm by means of eclipsing Z-scan experiments, J. Opt. Pure Appl. Opt. 9 (2007) L3.
[9] G. Ariyawansa, M.B.M. Rinzan, M. Strassburg, et al., GaN/AlGaN heterojunction infrared detector responding in 8–14 and 20–70μm ranges, Appl. Phys. Lett. 89 (2006) 14.
[10] R.B. Adamov, D. Pashnev, V.A. Shalygin, et al., Optical performance of two-dimensional electron gas and GaN:C buffer layers in AlGaN/AlN/GaN heterostructures on SiC substrate, Appl. Sci. 11 (2021) 6053.
[11] C.B. Lim, et al., Nonpolar m-plane GaN/AlGaN heterostructures with intersubband transitions in the 5–10 THz band, Nanotechnology 26 (2015), 435201.
[12] K. Feng, W. Streyer, S.M. Islam, et al., Localized surface phonon polariton resonances in polar gallium nitride, Appl. Phys. Lett. 107 (8) (2015), 081108.
[13] J.D. Caldwell, L. Lindsay, V. Giannini, et al., Low-loss, infrared and terahertz nanophotonics using surface phonon polaritons, Nanophotonics 4 (1) (2015) 44–68.
[14] L. Nordin, O. Dominguez, C.M. Roberts, et al., Mid-infrared epsilon-near-zero modes in ultra-thin phononic films, Appl. Phys. Lett. 111 (9) (2017), 091105.
[15] E. Shkondin, T. Repan, M.E.A. Panah, et al., High aspect ratio plasmonic nanotrench structures with large active surface area for label-free mid-infrared molecular absorption sensing, ACS Appl. Nano Mater. 1 (3) (2018) 1212–1218.
[16] T.G. Folland, G.Y. Lu, A. Bruncz, et al., Vibrational Coupling to epsilon-near-zero waveguide modes, ACS Photonics 7 (3) (2020) 614–621.
[17] A. Bile, M. Chauvet, H. Tari, et al., Supervised learning of soliton X-junctions in lithium niobate films on insulator, Opt. Lett. 47 (2022) 5893–5896.
[18] A. Bile, H. Tari, E. Fazio, Episodic memory and information recognition using solitonic neural networks based on photorefractive plasticity, Appl. Sci. 12 (2022) 5585.
[19] H. Tari, A. Bile, F. Moratti, et al., Sigmoid type neuromorphic activation function based on saturable absorption behavior of graphene/PMMA composite for intensity modulation of surface plasmon polariton signals, Plasmonics 17 (2022) 1025–1032.
[20] S.A. Biehs, Thermal heat radiation, near-field energy density and near-field radiative heat transfer of coated materials, Eur. Phys. J. B 58 (2007) 423–431.
[21] S. Fan, W. Li, Photonics and thermodynamics concepts in radiative cooling, Nat. Photonics 16 (2022) 182–190.
[22] M.E. Levinshtein, S.L. Rumyantsev, M.S. Shur (Eds.), Properties of Advanced Semiconductor Materials: GaN, AIN, InN, BN, SiC, SiGe, John Wiley & Sons, Hoboken, NJ, USA, 2001.
[23] T. Shaykhutdinov, A. Furchner, J. Rappich, et al., Mid-infrared nanospectroscopy of Berreman mode and epsilon-near-zero local field confinement in thin films, Opt. Mater. Express 7 (2017) 3706–3714.
[24] A.D. Dunkelberger, et al., Ultrafast active tuning of the berreman mode, ACS Photonics 7 (1) (2020) 279–287.
[25] N.C. Passler, et al., Second harmonic generation from phononic epsilon-near-zero berreman modes in ultrathin polar crystal films, ACS Photonics 6 (6) (2019) 1365–1371.
[26] N.C. Passler, A. Paarmann, Generalized 4×4 matrix formalism for light propagation in anisotropic stratified media: study of surface phonon polaritons in polar dielectric heterostructures, J. Opt. Soc. Am. B 34 (2017) 2128.
[27] A. Link, et al., Mater. Sci. Forum 353–356 (2001) 787–790.
[28] V. Tasco, et al., Investigation of different mechanisms of GaN growth induced on AlN and GaN nucleation layers, J. Appl. Phys. 105 (2009), 063510.
[29] I. Khan, Z. Fang, M. Palei, J. Lu, et al., Engineering the Berreman mode in the mid-infrared polar materials, Opt Express 28 (2020) 28590–28599.
[30] F. Bernardini, Fiorentini, Macroscopic polarization and band offsets at nitride heterojunctions, V. Physical Review B 57 (16) (1998) R9427.
[31] O. Ambacher, et al., Role of spontaneous and piezoeletric polarization induce effect in group-III nitride based heterostructures and devices, phys. stat. sol 216 (381) (1999) (b).